DOKUZ EYLUL UNIVERSITY
GRADUATE SCHOOL OF NATURAL AND APPLIED SCIENCES

PREPARATION AND CHARACTERIZATION OF CHITOSAN-CLAY BIOCOMPOSITES

by
Aylin ALTINIŞIK

July 2007
İZMİR

PREPARATION AND CHARACTERIZATION OF CHITOSAN-CLAY BIOCOMPOSITES

A Thesis Submitted to the
Graduate School of Natural and Applied Sciences of
Dokuz Eylul University
In Partial Fulfillment of the Requirements for
The Degree of Master of Science in Chemistry Program

by
Aylin ALTINIŞIK

July 2007
İZMİR

M. Sc. THESIS EXAMINATION RESULT FORM

We certify that we have read this thesis and **"PREPARATION AND CHARACTERIZATION OF CHITOSAN-CLAY BIOCOMPOSITES"** completed by **AYLİN ALTINIŞIK** under supervision of **PROF. DR. KADİR YURDAKOÇ** and that in our opinion it is fully adequate, in scope and in quality, as a thesis for the degree of Master of Science.

……..

Prof. Dr. Kadir YURDAKOÇ

Supervisor

…… ……..

Jury Member Jury Member

_____

Prof. Dr. Cahit HELVACI
Director
Graduate School of Natural and Applied Sciences

ACKNOWLEDGMENTS

The author is grateful to the supervisor of this thesis, Prof. Dr. Kadir YURDAKOÇ, for his valuable guide, help and advice, at all stages of this thesis study.

Also, I would like to thank to Inst. Dr. Yoldaş Seki for his precious suggestions and discussions during the preparation of the thesis.

In addition, I wish to express my gratefulness to all friends for their continuous helpful encouragement and valuable supports.

Finally, I would like to thank my family for bringing me in this situation with their unique patience and supports.

Aylin ALTINIŞIK

PREPARATION AND CHARACTERIZATION OF CHITOSAN-CLAY BIOCOMPOSITE

ABSTRACT

Chitosan-clay biocomposites have been prepared in which montmorillonite (MMT) is used as nanofiller and diluted acetic acid is used as solvent for dissolving and dispersing chitosan and montmorillonite respectively. The effect of MMT loadings in biocomposites has been investigated. The characterization with different methods (FTIR, DSC, TGA, and SEM) on chitosan/MMT biocomposites systems was examined. Morphology and properties of chitosan biocomposites have been studied compared with those of pure chitosan. The FTIR and SEM results indicated the formation of an intercalated-and-exfoliated structure at low MMT content and an intercalated-and-flocculated structure at high MMT content. The thermal stability and the mechanical properties of the composites were also examined by DSC, TGA/DTG and tensile strength measurements, respectively. The dispersed clay improves the thermal stability of the matrix systematically with the increase of clay loading. Tensile strength of a chitosan film was enhanced and elongation-at break decreased with addition of clay into the chitosan matrix.

Key words: Chitosan, biocomposite, montmorillonite, thermal properties

KİTOSAN KİL BİYOKOMPOZİTLERİNİN HAZIRLANMASI VE KARAKTERİZASYONU

ÖZ

Kitosan kil biyokompozitlerin hazırlanmasında nano-doldurucu olarak montmorillonit(MMT), kitosan ve kilin çözünmesi ve dağılmasında da seyreltik asetik asit çözücü olarak kullanılmıştır. MMT yüklemesinin biyokompozit üzerindeki etkisi araştırılmıştır. Kitosan/MMT biyokompozit sistemleri farklı karakterizasyon yöntemleriyle (FTIR, DSC, TGA ve SEM) incelenmiştir. Kitosan biyokompozitinin morfolojisi ve özellikleri saf kitosan ile karşılaştırılarak çalışılmıştır. FTIR ve SEM sonuçları, düşük MMT içerikli kompozit yapıların dağınık ve araya girmiş yapıda olduğunu ve yüksek MMT içerikli kompozit yapıların ise araya girmiş ve birikmiş yapıda olduklarını göstermiştir. Biyokompozitlerin termal kararlılıkları DSC ve TGA/DTG ile, mekanik özellikleri ise çekme deneyleriyle belirlenmiştir. Sonuç olarak kitosan matriksine kil eklenmesiyle kitosan filminin gerilme kuvveti artmış ve filmin esnemesi azalmıştır.

Anahtar Kelime: Kitosan, biyokompozit, montmorillonit, termal kararlılık

CONTENTS

Page

CHAPTER ONE

INTRODUCTION

1.1 Chitosan

1.1.1 The Properties of Chitosan

Chitosan (2-amino-2deoxy-(1→4)-β-D-glucopyranan), a polyaminosaccharide, normally obtained by alkaline deacetylation of chitin is the principal component of living organisms such as fungi and crustacean. When its DA (degree of N-acetylation) is lower than 50%, the chitin becomes soluble in aqueous acidic solution and is named chitosan. Up to the present time only a few cationic polymers exist and chitosan may be used as a flocculation and chelating polymer (Dung et al, 1994).

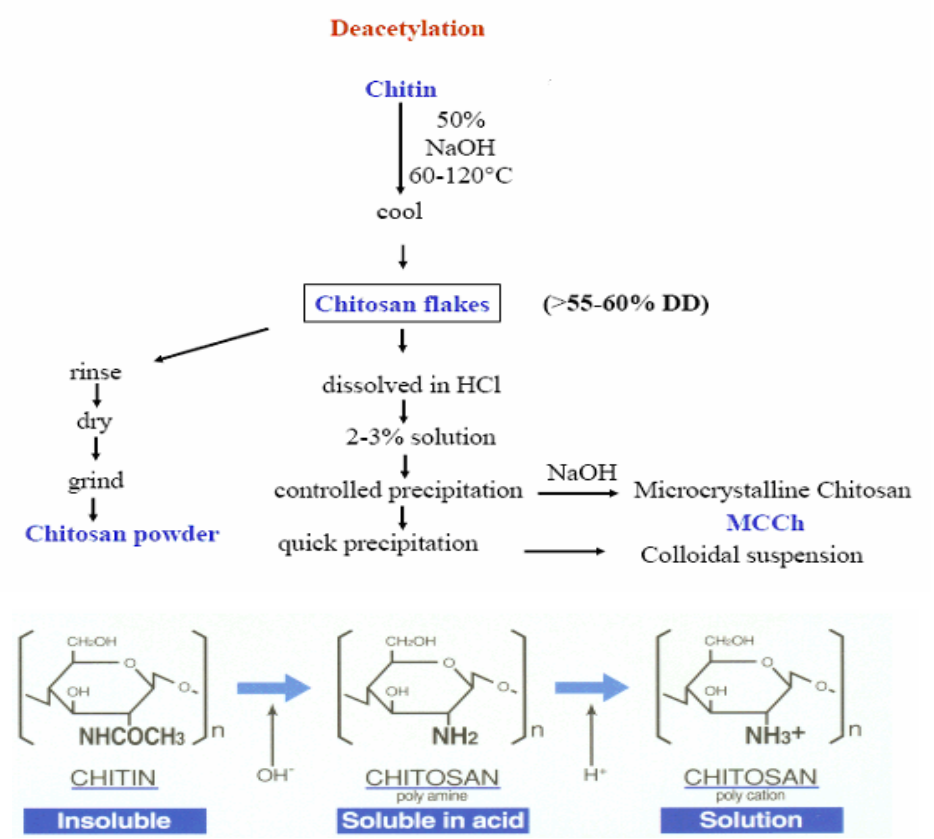

Figure 1.1 Deacetylation of chitin (www.kimica.jp/eng-chitosan-chemi-2.htm)

Chitosan a linear polymer of mainly anhydroglucosamine which behaves as a linear polyelectrolyte at acidic pH is nontoxic and bioabsorbable. At pH below 6.5, chitosan in solution carries a high positive charge density, one charge per glucosamine unit. Since chitosan is one of the few cationic polyelectrolytes, it is an exception to the current industrial high molecular weight polysaccharides, which are mostly neutral or polyanionic. It was documented that oral administration of chitosan with drugs enhanced their absorption from intestines into blood in animals. Chitosan is being evaluated in a number of biomedical applications including wound healing and dressing, dialysis membranes, contact lenses, fibers for digestible sutures, liposome stabilization agents, antitumor uses and drug delivery uses and controlled-release systems. In these uses chitosan's key properties are

- Biocompatibility
- Nonantigenicity
- Nontoxicity (its degradation products are known natural metabolites)
- The ability to improve wound healing/or clot blood
- The ability to absorb liquids and to form protective films and coatings, and
- Selective binding of acidic liquids, there by lowering serum cholesterol levels.

But chitosan has some drawbacks, it is only soluble in aqueous medium in the presence of a small amount of acid such as AcOH and its mechanical properties are not good for some biomedical application. Therefore many researchers tried to modify its properties (Sood and Panchagnula, 1998).

1.1.2 Applications of Chitosan

Applications of chitosan can be classified mainly in 3 categories according to the requirement on the purity of the chitosan:

1. Technical grade for agriculture and water treatment
2. Pure grade for the food and cosmetics industries
3. Ultra-pure grade for biopharmaceutical uses

1.1.2.1 Technical Grade for Agriculture and Water Treatment

Chitosan offers a natural alternative to the use of chemical products that are sometimes harmful to humans and their environment. In agriculture**,** Chitosan triggers the defensive mechanisms in plants (acting much like a vaccine in humans), stimulates growth and induces certain enzymes (synthesis of phytoalexins, chitinases, pectinases, glucanases, and lignin). This new organic control approach offers promise as a biocontrol tool. In addition to the growth-stimulation properties and fungi, chitosans are used for:

- Seed-coating
- Frost protection
- Bloom and fruit-setting stimulation
- Timed release of product into the soil (fertilizers, organic control agents, nutrients)
- Protective coating for fruits and vegetables

At the present time for water treatment, physicochemical-type treatment is widely used at potable and wastewater treatment plants. The major disadvantage of using synthetic chemical products is the risk of resulting environmental pollution. Treating wastewater using "greener" methods has become an ecological necessity. Chitosan, due to its natural origin and being biodegradable, has proven to be a most interesting alternative from several points of view.

Integrating a natural polymer made of crustacean residue into an existing system achieves a two-fold purpose: it improves the effectiveness of water treatment while reducing or even eliminating synthetic chemical products such as aluminum sulphate and synthetic polymers. Here are a few characteristics of chitosan that offer an ecological solution:

- Natural and biodegradable
- A powerful competitor for synthetic chemical products
- Potentially reduces the use of alum by up to 60% and eliminates 100% of the polymers from the treated water
- Improves system performance (suspended solids and chemical oxygen demand)
- Significantly reduces odor

1.1.2.2 Pure Grade for the Food and Cosmetics Industries

Chitosan is already used as a food ingredient in Japan, in Europe and in the United States as a lipid trap, an important dietetic breakthrough. Since chitosan is not digested by the human body, it acts as a fiber, a crucial diet component. It has the unique property of being able to bind lipids arriving in the intestine, thereby reducing by 20 to 30% the amount of cholesterol absorbed by the human body.

This raises the question: is chitosan really a "Fat Magnet"?

In solutions, chitosan has thickening and stabilizing properties, both essential to the preparation of sauces and other culinary dishes that hold their consistency well. Finally, as a flocculating agent, it is used to clarify beverages. Because of its phytosanitary properties, it can be sprayed in dilute form on foods such as fruits and vegetables, creating a protective, antibacterial, fungi static film. In Japan, a dilute solution of chitosan is commonly sprayed on apples and oranges as a protective measure. There are many other applications in the areas of nutraceutical and nutritional supplements, particularly for the broad range of chitosans that have been chemically or enzymatically modified.

Principal commercial applications include:

- Preservatives
- Food stabilizers
- Animal feed additives
- Anti-cholesterol additives (fat traps)

Chitosan forms a protective, moisturizing, elastic film on the surface of the skin that has the ability to bind other ingredients that act on the skin in cosmetics. In this way, chitosan can be used in formulating moisturizing agents such as sunscreens, organic acids, etc. to enhance their bioactivity and effectiveness. Today, chitosan is an essential component in skin-care creams, shampoos, and hairsprays due to its antibacterial properties.

Many patents have been registered and new applications are just beginning to appear including the most highly prized moisturizing and antibacterial properties. Applications include;

Maintain skin moisture:

- Treat acne
- Tone skin
- Protect the epidermis
- Reduce static electricity in hair
- Improve suppleness of hair
- Make hair softer

1.1.2.3 Ultra-Pure Grade for Biopharmaceutical Uses

For biopharmaceutical uses, it is in the field of health that the many properties of chitosan (bacteriostatic, immunologic, antitumoral, cicatrizant, hemostatic and anticoagulant) are of interest. For example, because of its biocompatibility with human tissue, chitosan's cicatrizant properties have proven its effectiveness as a component, notably, in all types of dressings (artificial skin, corneal dressings, etc.), surgical sutures, dental implants, and in rebuilding bones and gums. Applications currently being developed include artificial skin, surgical sutures that are absorbed naturally after an operation, and corneal contact lenses. Finally, chitosan delivers and time-releases drugs used to treat animals and humans. There are many potential chitosan applications in the health field but their development calls for the use of components that comply with strict pharmaceutical-grade requirements.

Possible applications include:

- Ointments for wounds
- Surgical sutures
- Ophthalmology
- Orthopedics
- Pharmaceutical products (delivery agent)
- Contact lenses looking forward.

Applications of chitosan are growing rapidly. Not only due to its multitude of applications but due to increasing environmental awareness of the population, biodegradable, and non-toxic products from 'natural' sources such as chitin and chitosan are going to be more and more appealing for the replacement of synthetic compounds. Moreover, in cosmetic and in biopharmaceutical industries, chitosan has exclusive properties which are not found in other synthetic products. (Contributed by Clermont Beaulieu, 2005)

1.2 CLAYS

1.2.1 General Definitions

Clay has two definitions. According to the clay mineralogist, a clay mineral is a layer silicate mineral (also called a phyllosilicate) or other mineral which imparts plasticity and which hardens upon drying or firing. (Guggenheim and Martin 1995) The word "clay" is also used to refer to a particle size in a soil or sediment. The term is used in the U.S. and by the International Society of Soil Science for a rock or mineral particle in the soil having a diameter less than 0.002 mm (2 microns), whereas sedimentologists classify particles smaller than 0.004 mm as clay (Seki, 2003).

In practice, "clay" is used to refer to the fine-grained, mineral fraction of earth material, and can include clay silicates as defined above, oxide-hydroxide minerals, such as goethite, hematite, manganese oxides, and some zeolites. Clay is used as a rock term and also as a particle – size term in the mechanical analysis of sedimentary rock, soils, etc. As a rock term it is difficult to define precisely, because of the wide variety of materials that have been called clays. In general the term clay implies a natural, earthy, fine-grained material which develops plasticity when mixed with a limited amount of water. By plasticity is meant the property of the moistened material to be deformed under the application of pressure, with the deformed shape being retained when the deforming pressure is removed. Chemical analyses of clays show them to be composed essentially of silica, alumina and water frequently with appreciable quantities of iron, alkali alkaline earths (Ralph E. Grim, 1968). In most cases clay finest as cheap filler have been used in polymer composites including rubbers, plastics, coatings and paints, etc. (Jing Cao Dai et al. 1999).

1.2.2 Classification of Clay Minerals

Clay minerals can be classified as indicated in scheme below (Rieder et al., 1998).

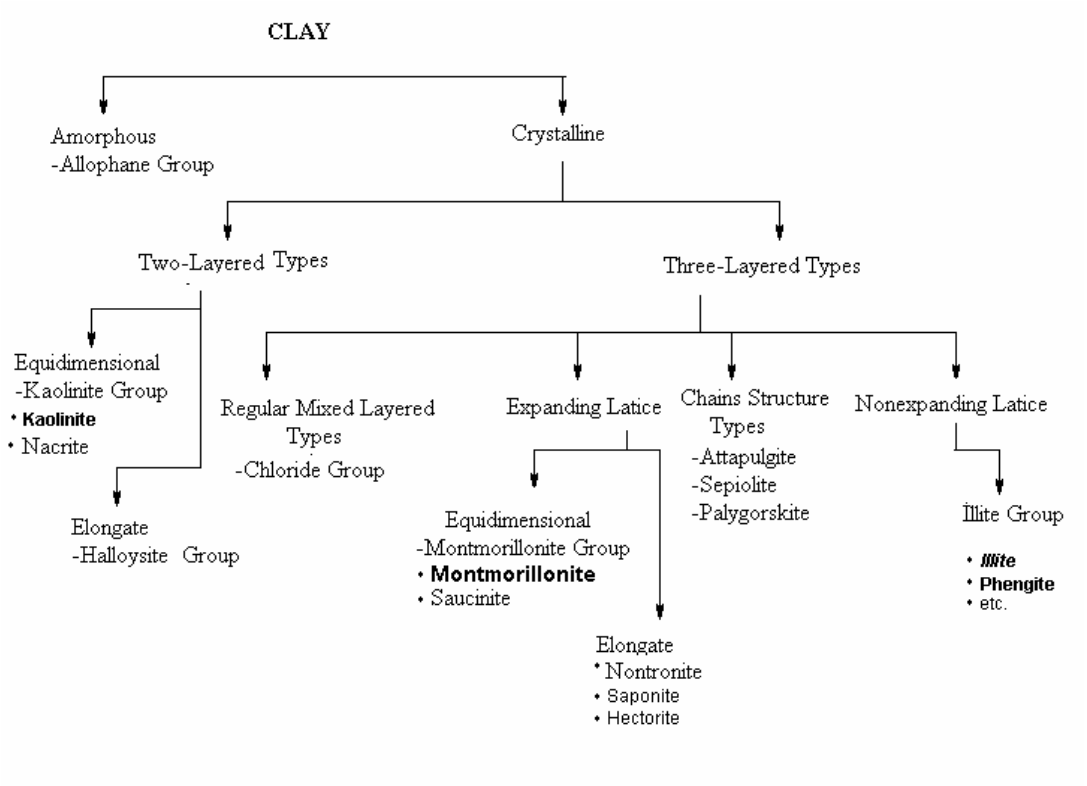

Figure 1.2 Classifications of Clay Minerals

1.2.3 Structure of the Clay Minerals

Two structural units are involved in the atomic lattice of most of the clay minerals (Ralph & Grim, 1968). The first unit is built of silica tetrahedrons. In tetrahedrons silicon atom is equidistant from four oxygen, or hydroxyl to balance the structure (As shown in Figure 1.1). Silicon atom is at the centre. Silica tetrahedral groups form hexagonal network. Silicon ion shares its charge equally between the four oxygen ions, leaving each oxygen with an excess charge of negative one. We now have the orthosilicate anion, which could at least theoretically be neutralized by four protons (hydrogen ions). This anion tends to react readily with alkali and alkali earth ions. The SiO_4^{4-} anion does have another option open to satisfy the charges.

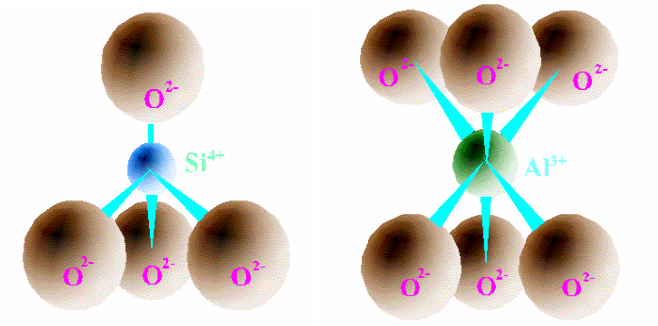

Figure 1.3 Silica tetrahedral unit and Octahedral unit (Seki, 2003)

The second unit is built of two sheets of closely packed oxygens or hydroxyls in which aluminium, iron, or magnesium atoms embedded magnesium, aluminium or iron atoms in octahedral co-ordination. When magnesium is present, all the positions are filled to balance the structure (Ralph and Grim, 1968). When aluminium is present, two- thirds of the suitable positions are filled to balance the structure as shown in Figure 1.3. Within the phyllosilicate mineral structure the aluminium ion is "more comfortable" in an octahedral co-ordination. The aluminium/oxygen radius ratio is 0.41. Aluminium might be said to share +0.5 of its charge with each of the surrounding oxygen ions, leaving each oxygen ion with a negative 1.5 charge.

Bentonite that is also known as montmorillonite derives from deposits of weathered volcanic ash. It often contains substantial amounts of magnesium and a wide variety of rare trace minerals. It is one of the most effective natural intestinal detoxifying agents available and has been recognized as such for centuries by native peoples around the world. Bentonite also selectively adsorbs an interesting variety of organic materials. Once hydrated (combined with water), bentonite has an enormous surface area. A single quart bottle can represent a total surface area of 960 square yards or 12 American football fields. Bentonite is made of a great number of tiny platelets, with negative electrical charges on their flat surfaces and positive charges on their edges. The application areas of bentonites vary depending on the kinds and amounts of its constituents such as smectites (which are the major clay minerals, other clay minerals) and non-clay minerals (Önal et al., 2001 Murray, 1991; Grim et al., 1978). When bentonite absorbs water and swells, it is stretched open like a highly

porous sponge; the toxins are drawn into these spaces by electrical attraction and bound fast. Bentonite can absorb pathogenic viruses, aflatoxin (a mold), and pesticides and herbicides including Paraquat and Roundup. The clay is eventually eliminated from the body with the toxins bound to its multiple surfaces.

Montmorillonite are dioctahedral smectites in which isomorphous substitution occurs. Aluminium and sometimes iron substitutes for silicon in the tetrahedral layer and iron or magnesium for aluminum in the octahedral layer (Newman, 1987) As a result of the isomorphous substitutions, crystalline order is reduced and structural imperfections arise (Seki, 2003)

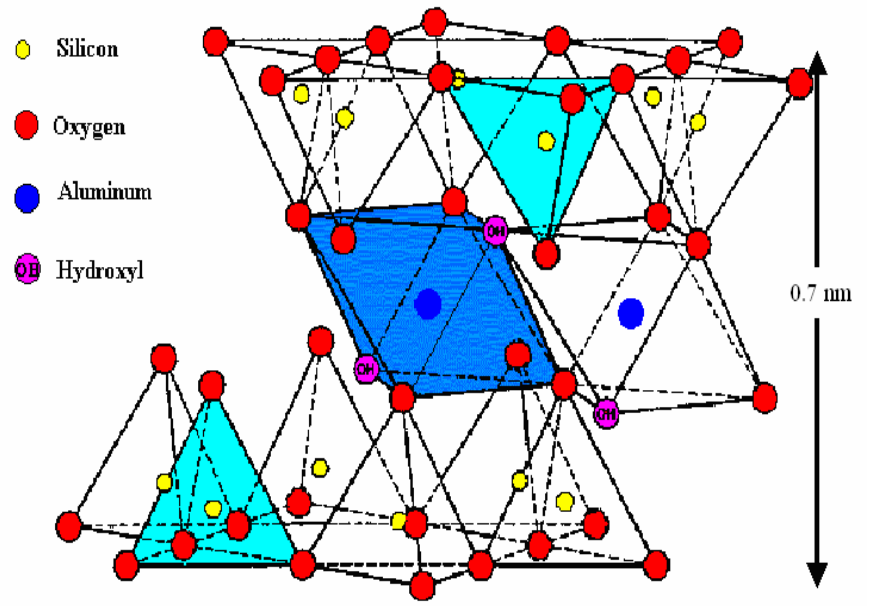

Figure. 1.4 The clay platelet is composed of silicon oxide units (highlighted in light blue) and aluminum oxide units (highlighted in dark blue). This structure repeats indefinitely, extending to the left and right, as well as into and out of the plane of the screen. (Seki, 2003)

1.2.4 Uses of clay minerals in health care and therapeutic products

Clay minerals are included in several health care formulations. In particular, they are presented in many semisolid preparations with different functions, including stabilization of suspensions and emulsions, viscosizing and other special rheological

tasks, protection against environmental agents, adhesion to the skin, adsorption of greases, control of heat release, etc. These functions are possible because of the special disposition of clay mineral particles when dispersed in polar solvents, due to their high surface areas and colloidal dimensions. When necessary, clays are processed or even modified to exalt or change some properties and new claylike materials with special features are also synthesized. Finally, clays are frequently used concomitantly with other rheological modifiers to obtain synergic effects, influencing the stability and/or other technical properties of the health care products (Viseras et al., 2006).

1.3. POLYMER / CLAY COMPOSITE

1.3.1 Dispersion of clay in polymer

Clays used in preparing polymer–clay composites belong to the 2:1 layered structure type. A member of the 2:1 family, montmorillonite is one of the most interesting and widely investigated clays for polymer nanocomposites. The structure of montmorillonite consists of layers made up of one octahedral alumina sheet sandwiched between two tetrahedral silica sheets, as shown in Figure 1.5.

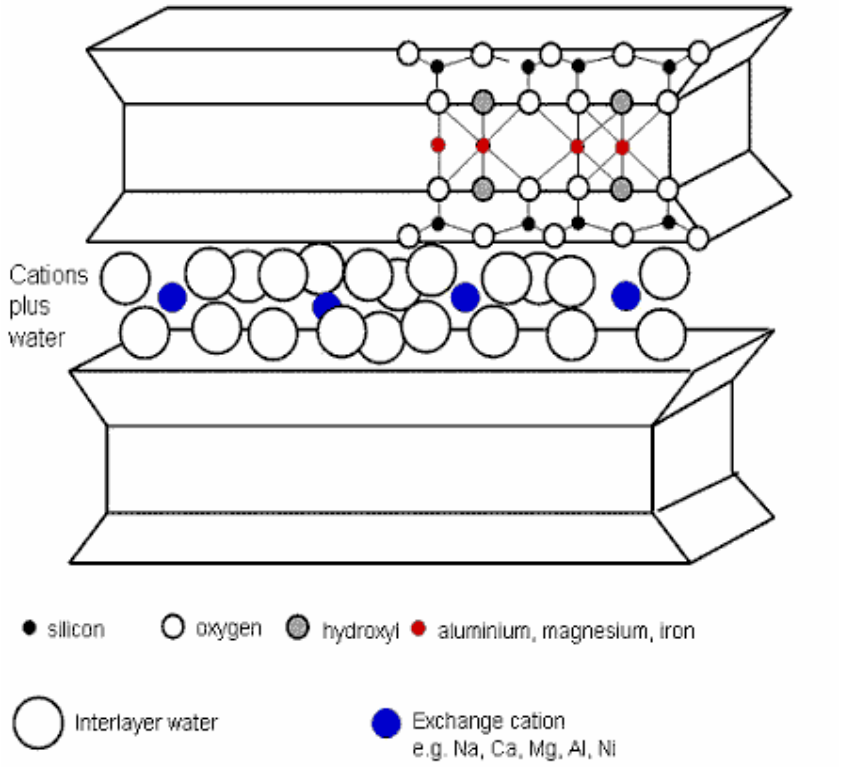

Figure 1.5 Idealized structure of a montmorillonite layer showing two tetrahedral-site sheets fused to an octahedral-site sheet (2:1 type). (Jill Geddes, n.d.)

Stacking of the silicate layers leads to a regular van der Waals gap between the layers. Approximately one in six of the aluminum ions in the octahedral layers of montmorillonite are isomorphously substituted by magnesium or other divalent ions.

The isomorphic substitution renders negative charges that are counterbalanced by cations residing in the interlayer. Pristine clay usually contains hydrated inorganic cations such as Na^{+}, K^{+}, and Ca^{+2}. When the inorganic cations are exchanged by organic cations such as from surfactants and polyelectrolytes, the clay surface changes its structure from hydrophilic to hydrophobic or organophilic (Theng, 1979 and 1974). The organic cations lower the surface energy and decrease the cohesive energy by expanding the interlayer distance, thus facilitating the wetting and intercalation of monomer or polymer. In addition, the organic cations may contain various functional groups that react with monomer or polymer resin to improve interfacial adhesion between clay nanolayers and polymer matrix.

Complete dispersion or exfoliation of clay tactoids in a monomer or polymer matrix may involve three steps similar to the dispersion of powders in liquids, as identified by Parfitt (Parfitt, 1981). The first step is wetting the surface of clay tactoids by monomer or polymer molecules. The second step is intercalation or infiltration of the monomer or polymer into the clay galleries, and the third step is exfoliation of clay layers. The first and second steps are determined by thermodynamics, while the third step is controlled by mechanical and reaction driving forces.

The dispersion of clay tactoids in a polymer matrix can result in the formation of three types of composites, as shown in Figure 1.6. The first type is a conventional composite that contains clay tactoids with the nanolayers aggregated in un-intercalated face-to-face form. In this case, the clay tactoids are dispersed simply as a segregated phase, resulting in poor mechanical properties of the composite.

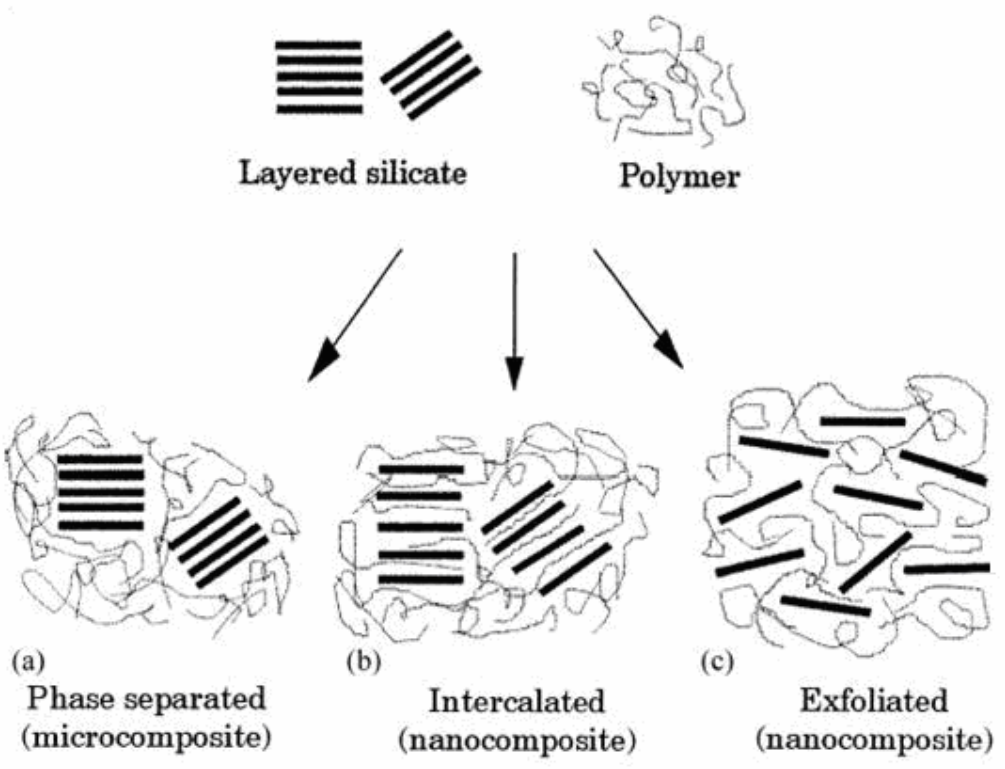

Figure. 1.6 Schematic of possible composite structures obtained when mixing polymer with Organoclays: (A) tactoids, (B) intercalation, and (C) exfoliation. (Yixiang Xu & Xi Ren & Milford A. Hanna, 2005)

The second type is intercalated polymer–clay nanocomposite, which is formed by the infiltration of one or more molecular layers of polymer into the clay host galleries. The last type is exfoliated polymer–clay nanocomposites, characterized by low clay content, a monolithic structure, and a separation between clay layers that depends on the polymer content of the composite. Exfoliation is particularly desirable for improving specific properties that are affected by the degree of dispersion and resulting interfacial area between polymer and clay nanolayers (Parfit, 1981).

1.3.2 Preparation Methods of Polymer / Clay Composite

1.3.2.1 Intercalation of Polymers or Pre-polymers from Solution

This technology is based on a solvent system in which polymers or pre-polymers are soluble and the silicate layers are swellable. The layered silicate is first swollen in a solvent such as water, chloroform, or toluene, etc. When the polymer and layered silicate solutions are mixed, the polymer chains intercalate and displace the solvent within the interlayer of the silicate. Upon solvent removal, the intercalated structure remains, resulting in polymer/clay nanocomposites.

1.3.2.2 The In Situ Intercalative Polymerization Method

In this method, the OMLS is swollen within the liquid monomer or a monomer solution so the polymer formation can occur between the intercalated sheets. Polymerization can be initiated either by heat or radiation, by the diffusion of a suitable initiator, or by an organic initiator or catalyst fixed through cation exchange inside the interlayer before the monomer swelling step.

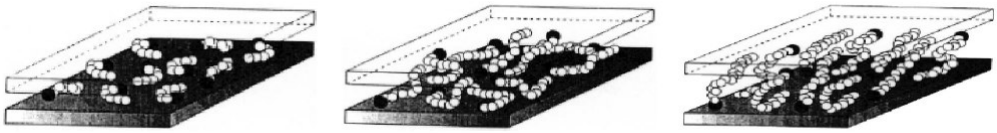

Figure 1.7 Alkyl chain aggregation models: (a) short chain lengths, where the molecules are effectively isolated from each other; (b) medium chain lengths, where quasi-discrete layers form with various degrees of in-plane disorder and interdigitation between the layers; and (c) long chain lengths, where interlayer order increases, leading to a liquid- crystalline polymer environment. Open circles represent the CH_2 segments while cationic head groups are represented by filled circles. (Okamoto 2004)

1.3.2.3 The Melt Intercalation Method

This method involves annealing, statically or under shear, a mixture of the polymer and OMLS above the softening point of the polymer. This method has great advantages over either *in situ* intercalative polymerization or polymer solution intercalation. First, this method is environmentally benign due to the absence of organic solvents. Second, it is compatible with current industrial processes such as extrusion and injection molding. The melt intercalation method allows the use of polymers which were previously not suitable for *in situ* polymerization or the solution intercalation method (Okamoto 2005).

1.3.3 Characterization of Polymer/Clay Composites *(Okamoto 2005)*

"The structure of polymer / clay nanocomposites has typically been established using a wide-angle x-ray diffraction (WAXD) analysis and transmission electron microscope (TEM) observations. Due to its availability and ease of use, WAXD is most commonly used to probe polymer / clay nanocomposite structures and, sometimes, to study the kinetics of the polymer melts intercalation. By monitoring the position, shape, and intensity of the basal reflections from the distributed silicate layers, the PLS nanocomposite structure (either intercalated or exfoliated) may be identified. For example, in exfoliated nanocomposites, the extensive layer separation associated with the delamination of the original silicate layers in the polymer matrix results in the eventual disappearance of any coherent x-ray diffraction from the distributed silicate layers. On the other hand, for intercalated nanocomposites, the finite layer expansion associated with the polymer intercalation results in the appearance of a new basal reflection corresponding to the larger gallery height.

WAXD offers a convenient method to determine the interlayer spacing of the silicate layers in the original layered silicates and in the intercalated nanocomposites (within 1–4 nm), but little can be said about the spatial distribution of the silicate layers or any structural in homogeneities in the PLS nanocomposites. Additionally, some layered silicates initially do not exhibit well defined basal

reflection. Thus, peak broadening and intensity decreases are very difficult to study systematically. Therefore, only tentative conclusions can be drawn concerning the mechanism of nanocomposite formation and their structure based solely on WAXD patterns.

On the other hand, TEM allows a qualitative understanding of the internal structure, spatial distribution of the various phases, and defect structure of nanocomposites through direct visualization. However, special care must be exercised to ensure that a representative cross section of the sample is evaluated. The WAXD patterns and corresponding TEM images of three different types of nanocomposites are presented in Figure 1.7. (Okamoto, 2005)".

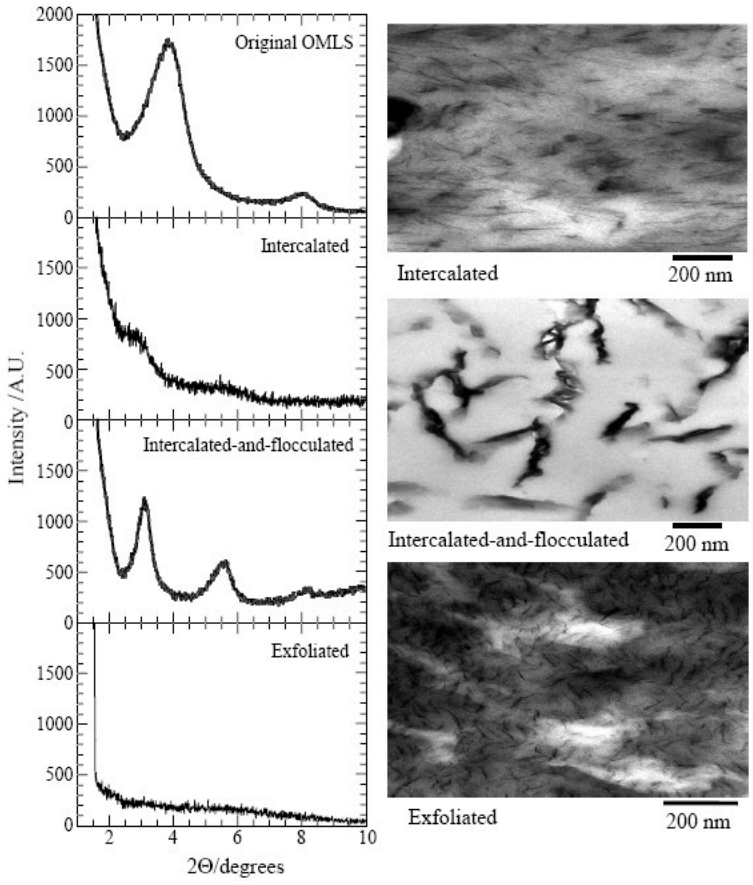

Figure 1.7 (a) WAXD patterns, (b) TEM images of three different types of nanocomposites. (Masami Okamoto, 2005)

1.4 PURPOSE OF THE STUDY

Chitosan has been extensively investigated for several decades for molecular separation, food packaging film, artificial skin, bone substitutes, water engineering and so on, owing to its good mechanical properties, biocompatibility, biodegradability, multiple functional groups as well as solubility in aqueous medium. However, its properties, such as thermal stability, hardness and gas barrier properties are frequently not good enough to meet those wide ranges of applications. Up to now, there is only a limited number of reports about the enhancement of properties of chitosan using PLSNs technology.

The aim of the present study is to prepare high-performance chitosan by incorporating montmorillonite. The effect of MMT on the rheological and colloidal properties of chitosan biocomposite dispersions at different MMT concentrations will also be examined. The hydrogen bonding force between chitosan and MMT and clay loading on the morphology, thermal stability and mechanical properties of the nanocomposites have been investigated. The structural analysis of chitosan/MMT biocomposite materials will be studied using FTIR, SEM, mechanical testing. The thermal behaviour of the biocomposite will be determined by using TGA and DSC.

CHAPTER TWO

MATERIALS AND METHODS

2.1 Materials

Chitosan (highly viscous) was purchased from Fluka (degree of deacetylation: 75-85%, average molecular weight: 500000-700000 g mol^{-1}) as a flaked material. Acetic acid (HAc) and sodium hydroxide (NaOH) were obtained from Riedel de Haen.

KSF montmorillonite was supplied from Fluka.

2.2 Preparation of the biocomposites

Chitosan solution was prepared by dissolving chitosan (CS) in a 2% (v/v) aqueous acetic acid solution at a concentration of 2 wt% followed by filtering to remove the insoluble material. MMT was first swelled by 50 mL distilled water and then added to 50 ml chitosan solution with MMT contents of 1wt%, 2 wt%, 5 wt%, followed by stirring at 60 °C for 6 h. After that, MMT/CS solutions were cast on a petri dish at 60 °C for 48 h. The dry films still contained a small quantity of the solvent (HAc), which formed chitosonium acetate. After drying, the films were soaked in 1 M aqueous NaOH for 5 h to neutralize the acid followed by rinsing in distilled water to neutral and then dried at vacuum oven at 60 °C for 24 h. They were termed CS-x which is the content of MMT.

All the biocomposite films were dried at 60 °C for overnight before testing and the neat CS films were made in the same conditions as their biocomposites. The thermal stability and mechanical properties of chitosan and the biocomposites were compared with each other.

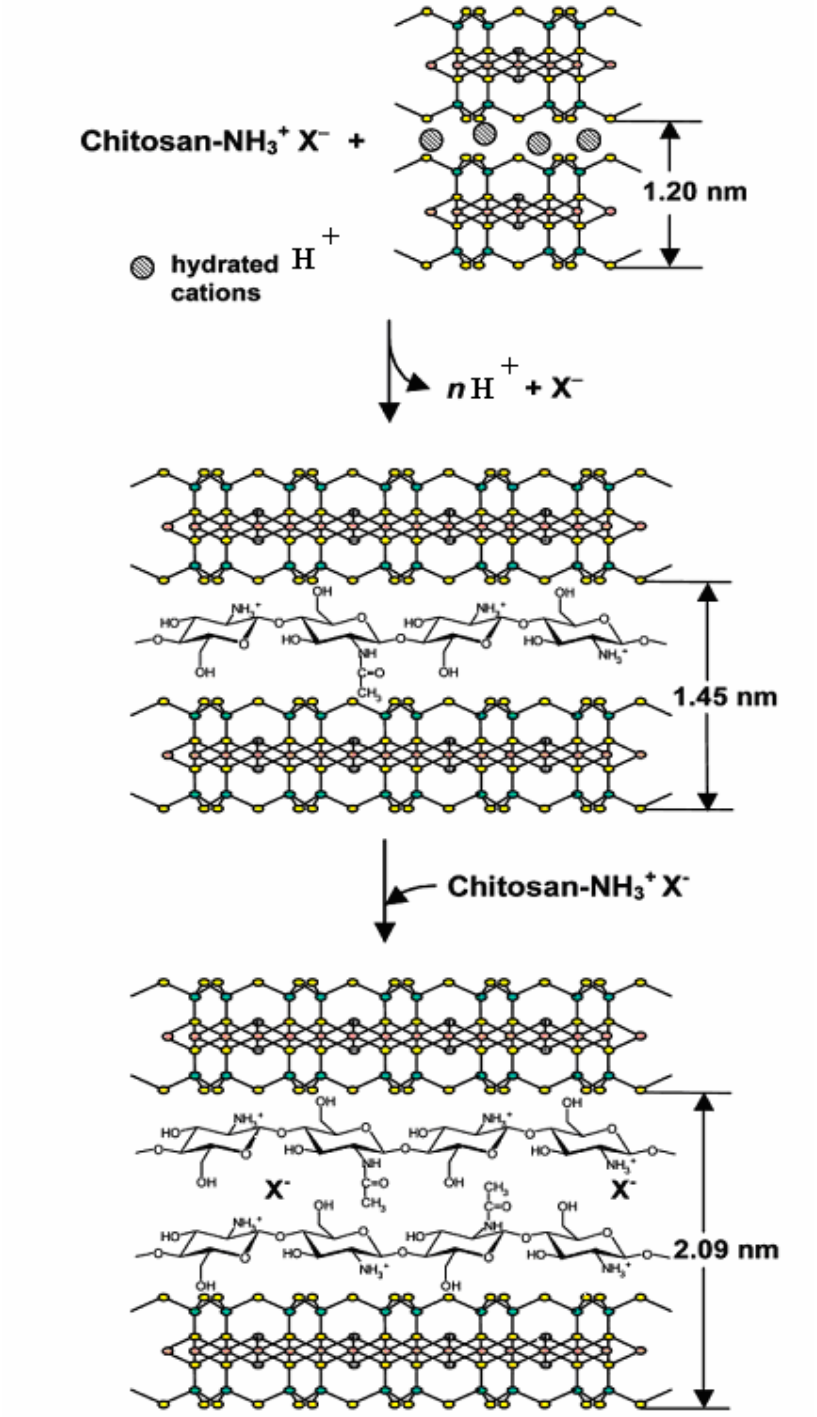

Figure 2.1 Chitosan-clay interaction mechanism (Margarita Darder & Montserrat Colilla & Eduardo Ruiz Hitzky, 2003)

2.3 Characterization of Biocomposites

2.3.1 Fourier Transform Infrared (FTIR) spectra of the samples

FTIR spectroscopy was used to obtain the information about the interactions between chitosan and clay sample. Chitosan film, MMT and biocomposites were brought to constant weight in a drying oven at 60 ºC for 24 h.

Fourier transform infrared (FTIR) spectra (transmission) were measured on a Perkin-Elmer FTIR spectrophotometer Spectrum BX-II in the range 4000-400 cm^{-1} at a resolution of 4 cm^{-1}.

2.3.2. Thermal Analysis

Differential scanning calorimetry (DSC) of Chitosan and its biocomposite in the temperature range of 5-500˚C were performed at a heating rate of 10˚C/min under Ar flow of 10 mL min^{-1} in SETARAM DSC Model 111 in Darmstadt Technical University, Ernst-Berl Institute, Department of Industrial Chemistry/Germany.

The thermal properties of biocomposites and pure chitosan were investigated by thermogravimetric analysis (TGA). TGA was performed under nitrogen flow and atmosphere air from room temperature to 800˚C at a rate of 20˚C/min with a Perkin Elmer Diamond TG/DTA instrument. The weights of samples varied from 2 to 3 mg.

2.3.3 SEM Analysis

The surface morphologies of the composites were studied using a scanning electron microscope at an accelerating voltage of 20 kV. All samples were dried and coated with gold before scanning to increase conductivity. SEM photographs were taken at different magnifications (in the range of 1000X and 5000X) by using Jeol JSM 60 model SEM apparatus equipped with energy dispersive X-Ray (EDX) in Metallurgy and Materials Engineering Department of Dokuz Eylül University/Izmir.

2.3.4 Mechanical Testing

Tensile strength (TS) and elongation at-break (E) were measured with an Testing Machine (Model AG-I 10 kN, Shimadzu, Japan) following the guidelines of ASTM Standard Method D 882–91 (ASTM., 1995).

The initial grip separation was set at 20 mm and the crosshead speed was set at 200 mm/min. TS was expressed in MPa and calculated by dividing the maximum load (N) by the initial cross sectional area (m^2) of the specimen. E was calculated as the ratio of the final length at the point of sample rupture to the initial length of a specimen (20 mm) and expressed as a percentage. TS and E tests were replicated three times for each type of film.

CHAPTER THREE

RESULTS AND DISCUSSION

3.1 Fourier Transform Infrared (FTIR) Spectra of the Samples

The structure of the chitosan biocomposites particles was analyzed by using FTIR spectroscopy. Figure 3.1 A–E shows FTIR spectra of MMT/chitosan biocomposites and MMT dispersions. The spectrum of MMT shows the characteristic bands 3625 cm^{-1} due to O–H stretching, a broad peak centered on 3407 cm^{-1} due to interlayer and interlayer H-bonded O–H stretching, 1633 cm^{-1} due to H–O–H bending 1045 cm^{-1} due to Si–O stretching, 916 cm^{-1} due to Al–OH, and 529 and 479 cm^{-1} due to Si–O bending vibrations (Alemdar et al., 2005; Marel & Beutelspacher, 1976). The exchange of simple inorganic cations by the other ions results in the enhancement of the intensity of the 3500–3200 cm^{-1} band along with a reduction of intensities due to Si–O and Al– O. The increase in intensity of the 3500–3200 cm^{-1} band reflects the increased hydrogen bonding between the lattice hydroxyls and organic groups. When the protons in chitosan are hydrogen-bonded to the oxygen species of Si–O and Al–O segment, Si–O and Al–O bonds would be weakened and the tetrahedral symmetry of these moieties will be distorted. On the other hand, FTIR analysis shows that the MMT/chitosan composites exhibited resolved N–H, O–H, and C–H bands when the composites are formed. The chitosan composites show three stretching vibration regions: N–H and O–H from chitosan, and O–H, Si–O, (Al, Mg)–OH, or Al–OH from the MMT. This would result in the change of the IR band positions as well as the reduction of intensities of the bands. It can clearly be seen that the chitosan adsorbed MMT spectra; exhibit the presence of characteristic absorptions due to the organic and inorganic groups.

While standard chitosan showed bands at 2914 and 2897 cm^{-1} (aliphatic C–H stretching), 1379 cm^{-1} and 1414 cm^{-1} (C–H bending), 1651 cm^{-1} and 1538 cm^{-1} (N–H bending), 1152 and 1089 cm^{-1} (C–O stretching), and the infrared spectra of Cs-1 (MMT/chitosan) biocomposites (Figure.3.1) showed additional bands including 1652

cm^{-1} and 1572 cm^{-1} (N–H bending), 1416 and 1377 cm^{-1} (C–H bending), and also absorbencies due to structural O–H stretching at 3521 cm^{-1} and Al–O vibrations at 912, 639 and 489 cm^{-1} confirm the presence of MMT in the dispersion. In the MMT chitosan adsorption products, the structural O–H stretching band was broadened and gave a maximum at 3521 cm^{-1}, and the Si–O stretching bands were also given a maximum at 1070 cm^{-1} and finally Si–O bending peak was changed to 489 cm^{-1}.

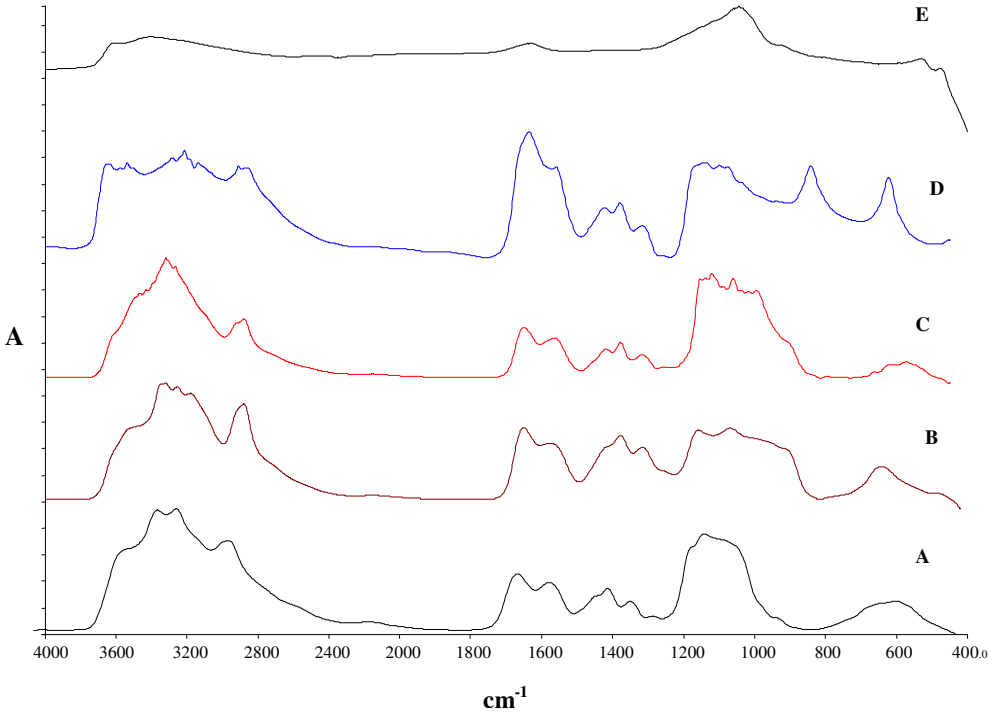

Figure 3.1 FTIR spectrum of : (A) Chitosan, (B) Cs-1, (C) Cs-2, (D) Cs-5, (E) MMT

The spectrum of Cs-2 (MMT/chitosan) biocomposite also contains characteristic bands of all components. These results showed that the chitosan molecules and clay particles mainly interact on the surface each other.

In addition, the intensities of the Al–O bands and structural O–H stretching vibrations also decrease in the order MMT < Cs-5 < Cs-2 < Cs-1. This is attributed to the relaxation of hydrogen bonding between (Al–O) O–H deformations as well as to the hydrated water of exchangeable cationic metal ions on the montmorillonite.

Figure 3.1 shows the FTIR spectra for Cs, Cs-1, Cs-2 and Cs-5 clearly show the bands (1538 cm^{-1}, 1572 cm^{-1}, 1565 cm^{-1} and 1558 cm^{-1}), which corresponds to the deformation vibration of the protonated amine group (-NH3 $^{+}Ac^{-}$) in chitosan, while Cs, Cs-1, Cs-2 and Cs-5 show the band which corresponds to the -NH_2 group.

Table 3.1 Results of FTIR spectra of the samples

	υ_{OH} (cm^{-1})		υ_{CO} (cm^{-1})	υ_{NH} (cm^{-1})		υ_{CH} (cm^{-1})	
	stretching	bending	stretching	stretching	**bending**	stretching	bending
MMT	3625	1633	-	-	-	-	-
Cs	3511	Not observed	1152-1089	3305	***1651-1538***	2914-2897	1379-1414
Cs-1	3521	Not observed	1163-1072	3353	***1652-1572***	2906-2876	1416 1377
Cs-2	3568	Not observed	1119-1060	3484	***1648-1565***	2878	1417-1378
Cs-5	3642	Not observed	1137-1099	3536	***1634-1558***	2904-2853	1422-1381

3.2 Thermal Analysis

3.2.1 Thermogravimetric Analysis (TGA)

The thermal stability of the chitosan and its biocomposites has been investigated by TGA under both nitrogen and air flows (Figure 3.2 and 3.3). On the TGA curves, one can see that the degradation of chitosan and its biocomposite in the nitrogen and air flows are different. Under nitrogen flow, a non-oxidative degradation occurs, while the use of air allows oxidative degradation of the samples. Under nitrogen flow, there are two steps of degradation. The first range (25-200°C) is associated with the loss of water about 6-8 wt%, whereas the second range (210-410°C) corresponds to the degradation and deacetylation of chitosan and left about 40 wt% solid residue.

In air flow, there is another degradation step (410-580°C), which may be assigned to the oxidative degradation of the carbonaceous residue formed during the second step. From Figure 3.3, 3.5 and Table 3.3, it is clearly observed that the degradation mechanism of CS and its biocomposites.

The dispersed clay in the chitosan matrix exhibits a significant delay in weight loss, especially at high temperature (>400°C). After pyrolysis, the nanocomposite forms char with a multilayered carbonaceous-silicate structure, which may keep its multilayered structure in the polymer matrix even at 600°C (Wang, 2002). This high-performance carbonaceous-silicate char builds up on the surface during burning, thus insulating the underlying material and slowing the escape of the volatile products generated during decomposition.

The dispersed lamellae of clay in polymer matrix will result qualitatively in a spatially more uniform and thicker char during decomposition. The dispersed clay enhances the formation of char on the surface of polymer matrix and as a consequence, reduces the rate of decomposition (Gilman JW., 1999 and Vaia RA, Price G, Ruth PN, Nguyen HT, Lichtenhan, 1999). The thermal stability of the biocomposites increases systematically with increasing clay, up to loading of 5 wt%.

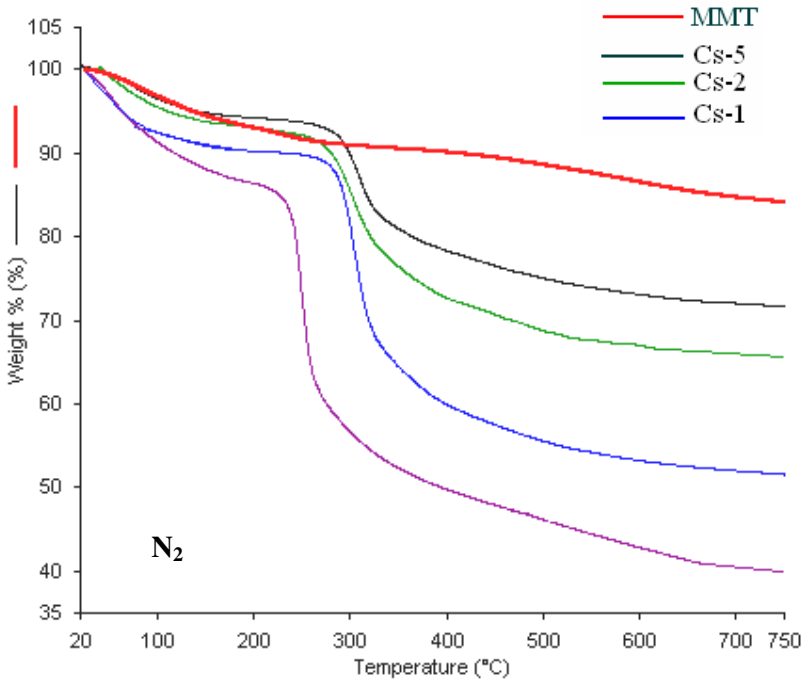

Figure 3.2 Thermogravimetric curves of montmorillonite, chitosan and its nanocomposites: MMT, CS, CS-1, CS-2 and CS-5 in nitrogen flow;

Table 3.2 Results of thermogravimetric analysis in nitrogen flow

Sample	First stage		Second stage		Weight % remaining after 600°C
	T (°C)	Weight lost %	T (°C)	Weight lost %	
Cs	56	13.4	250	37.9	42.6
Cs-1	64	10.4	301	35.6	53.5
Cs-2	66	6.7	303	26.7	66.9
Cs-5	78	6.3	308	17.4	73.0

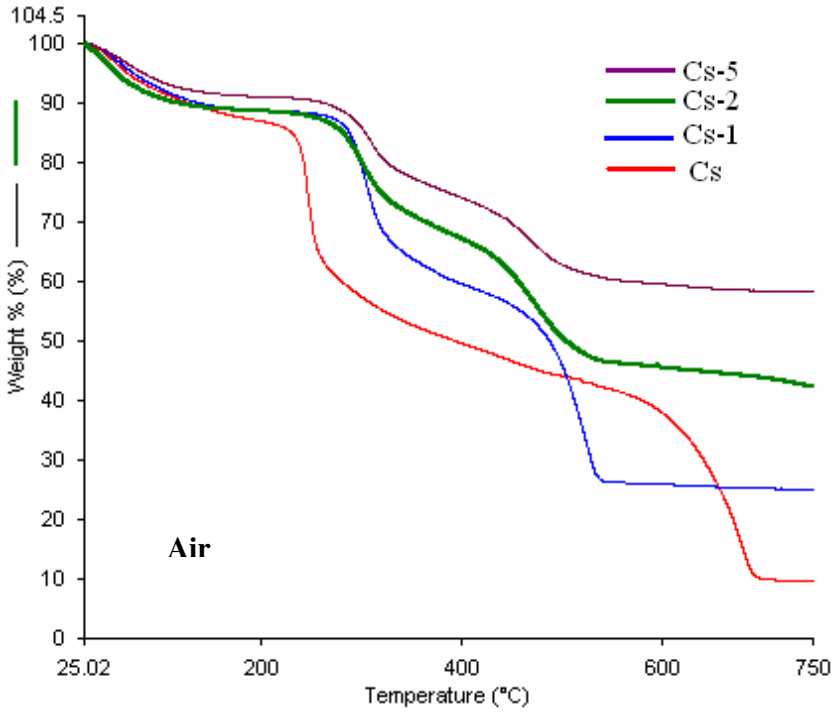

Figure.3.3 Thermogravimetric curves of chitosan and its nanocomposites: CS, CS-1, CS-2 and CS-5 in atmosphere air.

Table 3.3 Results of thermogravimetric analysis in atmosphere air

Sample	First stage		Second stage		Third stage		Weight remaining after 700°C
	T (°C)	Weight lost %	T (°C)	Weight lost %	T (°C)	Weight lost %	
Cs	59	12.9	248	37.7	676	32.3	10.4
Cs-1	66	11.3	304	29.6	512	32.9	26.4
Cs-2	68	11.3	302	20.9	475	21.7	44.0
Cs-5	72	9.1	310	16.6	468	14.6	58.5

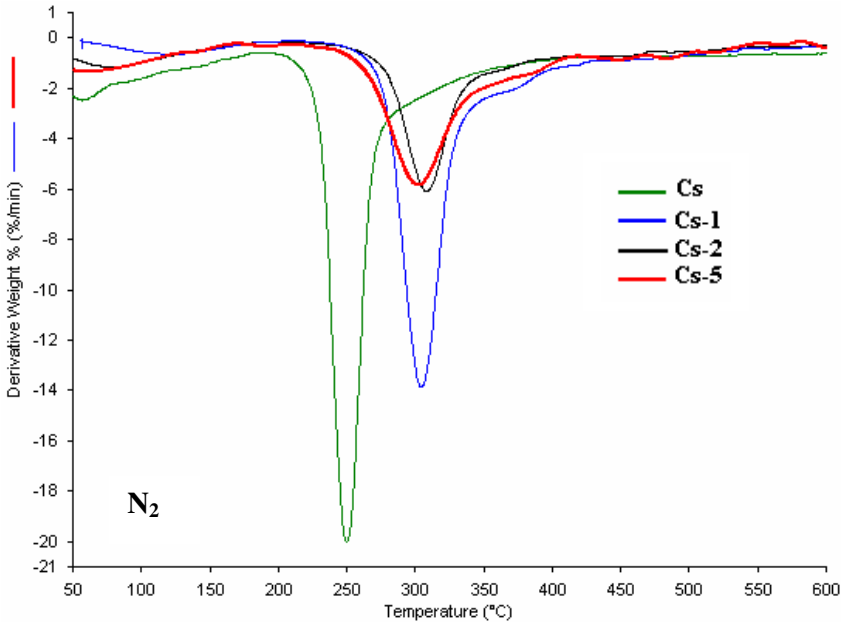

Figure 3.4 DTG curves of chitosan and its nanocomposite under nitrogen flow

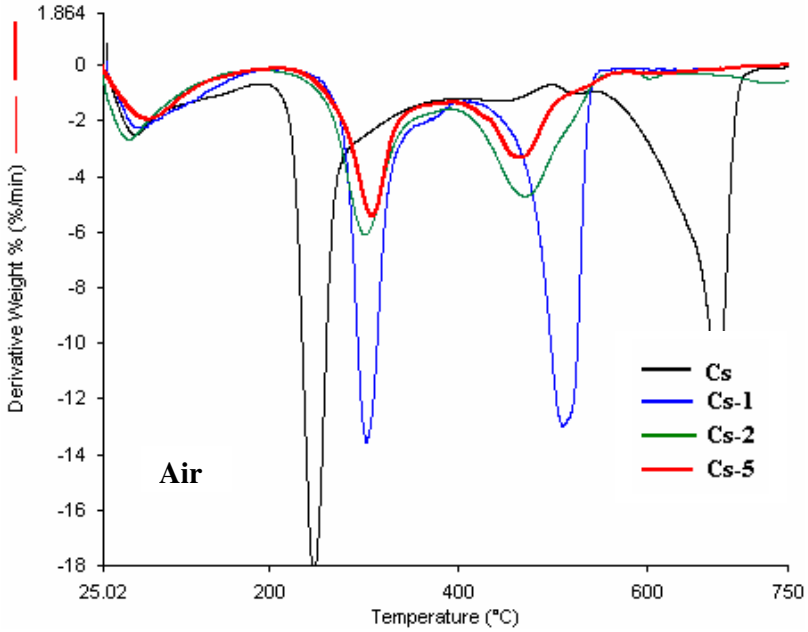

Figure 3.5 DTG curves of chitosan and its nanocomposite under atmosphere air.

3.2.2 Differential Scanning Calorimeter (DSC)

The thermal properties of chitosan and its biocomposites have been studied using DSC from 20°C to 500°C. The DSC thermograms of Chitosan, Cs-1, Cs-2 and Cs-5 were given in Figure 3.6. As shown by DSC analysis of Chitosan in Figure 2.2.1, an endothermic peak at 93°C represents melting endothermic peak of Chitosan. The melting endothermic peak of its biocomposites were observed at 90°C, 121°C and 115°C for Cs-1, Cs-2 and Cs-5 respectively. As can be seen from these results intercalated of Chitosan with clay melting temperatures were increased. In addition to this, as the amount of clay in Chitosan was increased, melting points of hydrogels also increased.

The exothermic peaks in Figure 3.6 were observed due to thermal decomposition. For Chitosan the exothermic peaks were seen at 309°C. However exothermic peaks representing thermal decomposition of its nanocomposites were appeared to be 300°C, 296°C and 304°C for Cs-1, Cs-2 and Cs-5. It is clear that the temperature of the exothermic peak of Chitosan was higher than those of its biocomposite.

The glass transition temperature (T_g) can usually be obtained by DSC. The glass transition temperature of chitosan is still a subject of controversy. The main reason may be that, being a natural polymer, some properties like crystallinity, molecular weight and deacetylation degree, can present wide variations according to the source and/or method of extraction and will influence the T_g. (Ratto et al., 1995) The observed glass transition temperature of chitosan for water contents ranging from 8 to 30% was 30 °C (Lazaridou and Biliaderis, 2005). It has found that T_g of chitosan with its water content ranging from 23 to 67 °C due to the plasticizing effect of water. On the other hand, observed that T_g of chitosan at 203 °C (Sakurai, Maegawa, and Takahashi, 2000). In another reference, it was found no evidence for Tg suggesting that T_g of chitosan at which lies at a higher temperature, where degradation prevents its determination (Kittur et al., 2002).

In the present study the DSC measurements showed no significant stepwise increase in specific heat, showing, therefore, no evidence in favor of the occurrence of a glass transition temperature.

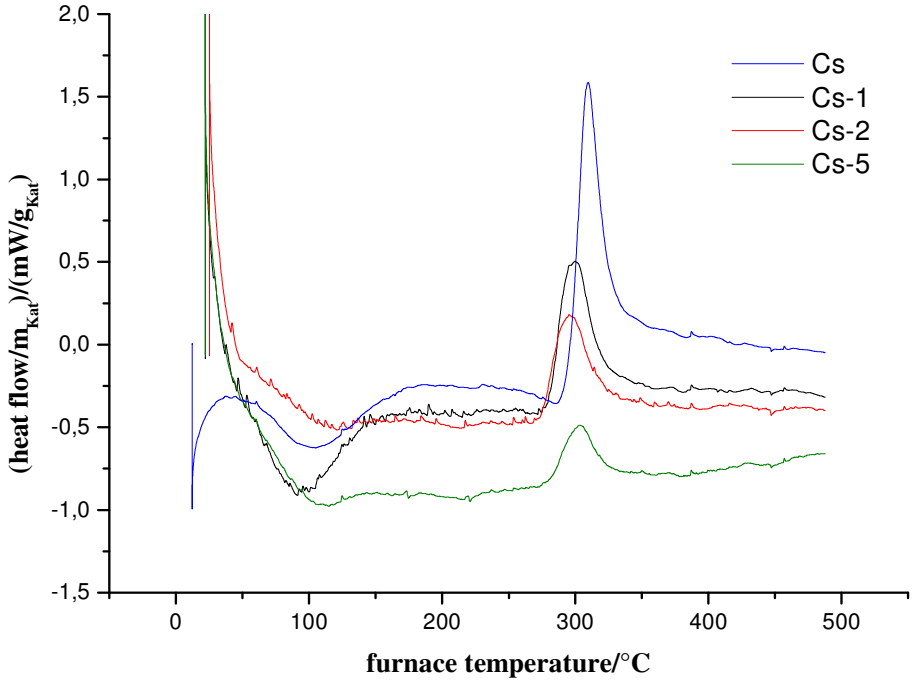

Figure 3.6 DSC thermographs of chitosan-clay nanocomposites with different MMT contents.

Table 3.4 Results of DSC analysis

Materials	T_m (°C)	T_d (°C)
Cs-1	90	300
Cs-2	121	296
Cs-5	115	304

3.2.3 Scanning Electron Microscopy Analysis (SEM)

In order to investigate clay aggregation in the chitosan matrix, surface morphology of clay biocomposites were studied by using SEM analysis. SEM results were presented in Figure 3.7 which compares between the microscopic surfaces of clay biocomposites containing 1, 2, and 5 % montmorillonite.

SEM images, it is clearly illustrated that the MMT keeps intercalated and exfoliated structures at lower MMT content, while with the increasing of MMT content, the MMT layers assemble to form intercalated and flocculated structures. It is believed that the formation of flocculated structure in Cs/MMT biocomposites is due to the hydroxylated edge-edge interaction of the silicate layers (Ray and Okamoto, 2003). Since one chitosan unit possesses one amino and two hydroxyl functional groups, these functional groups can form hydrogen bonds (see Figure 2.1) with the silicate hydroxylated edge groups, which lead to the strong interaction between matrix and silicate layers. This strong interaction is believed to be the main driving force for the assembly of MMT in the CS matrix to form flocculated structure.

The results show that the use of chitosan promoted the clay disaggregation as well as its better homogenous dispersion in chitosan matrix.

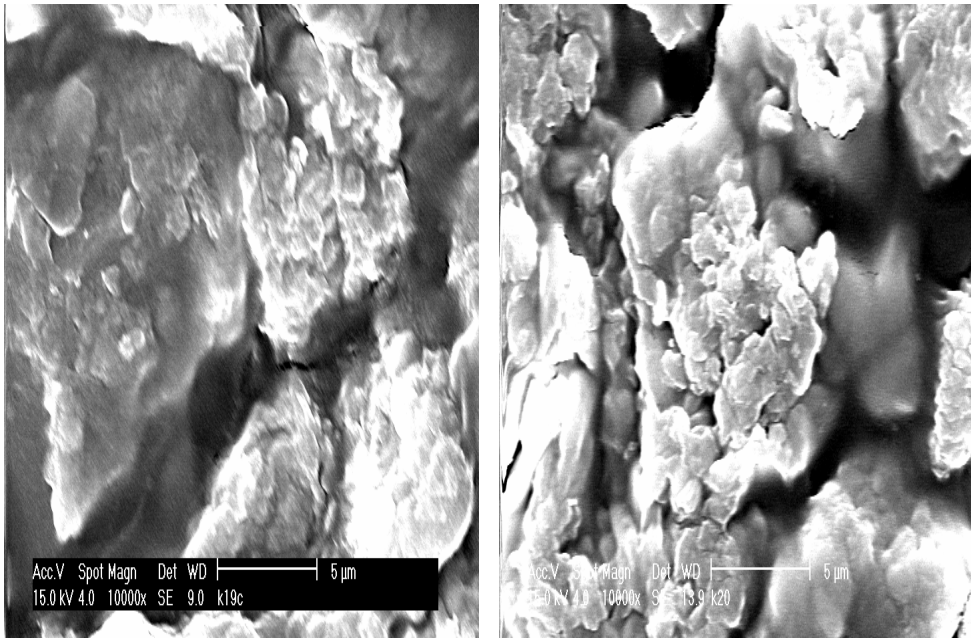

A B

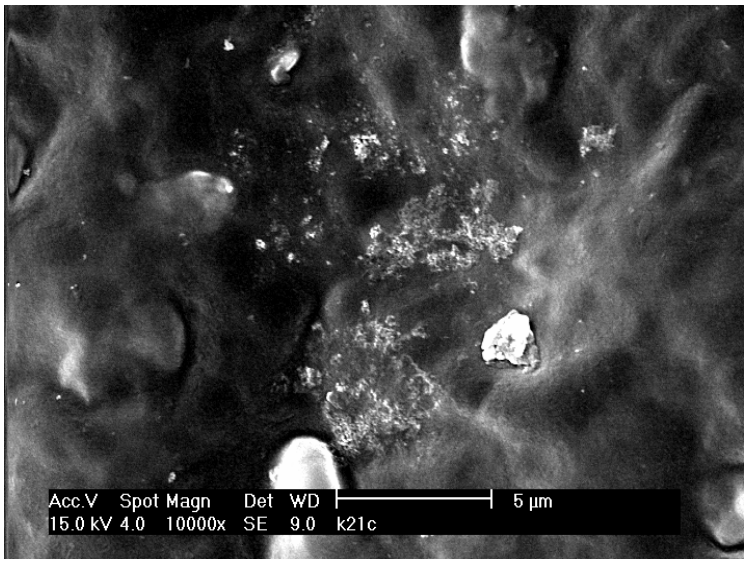

C

Figure 3.7 SEM images showing the surface morphologies of the biocomposites (A) Cs-1, (B) Cs-2,(C) Cs-5.

3.2.4 Mechanical Properties

The mechanical properties of chitosan and chitosan/ clays biocomposite films were measured and are summarized in Table 3.5. The pure chitosan film had a TS of 21.4 MPa and an E of 10.0 %. The TS of biocomposite films increased significantly with increasing amount of MMT up to 2 wt %, followed by a decrease with further increase in MMT up to 5 wt %. When 1 wt % MMT was added, the TS of the biocomposite film was 23.3 MPa, an approximately 9 % increase compared with that of pure chitosan film. TS were the highest for 2 wt % clay hybrid, in which 18 % improvement was observed. Further increasing clay content to 5 wt % decreased TS of the film to 18.9 MPa.

E of the composite film decreased slightly with addition of MMT. The substantial enhancement of TS with the addition of a small amount of MMT was ascribed to formation of an exfoliated state and the uniform dispersion of MMT in the chitosan matrix (Misra, and M. Park, and H. Mohanty and A. K. Drzal, 2004; Zheng and J. P. Li and P. Ma, and Y. L. Yao and K. D. J 2002). It was also attributed to strong interaction between chitosan and MMT (Choi et al, 2003). The decrease in TS with increasing MMT content up to 5 wt % resulted from the aggregation of MMT particles with high surface energy when the MMT content was high enough (Misra et al, 2004)

Table 3.5 Mechanical Properties of Chitosan/clay nanocomposites

Materials	**Tensile strength (MPa)**	**Elongation at break (%)**
Cs	21.4	10.0
Cs-1	23.3	8.0
Cs-2	26.1	7.9
Cs-5	18.9	5.7

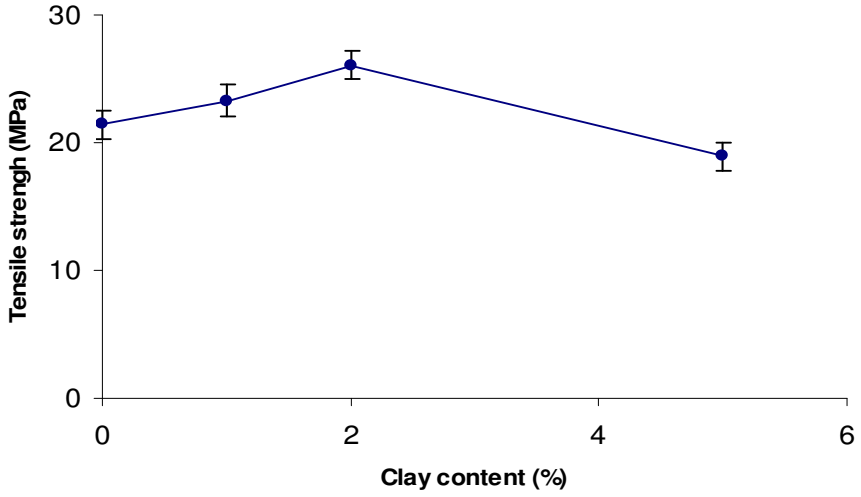

Figure.3.8 Effect of MMT content on tensile strength (The error bars represent the standard errors of mean (SEM)).

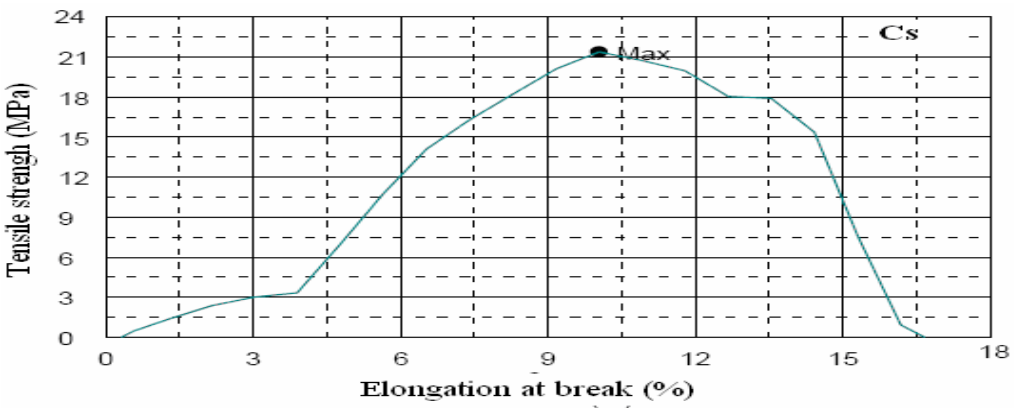

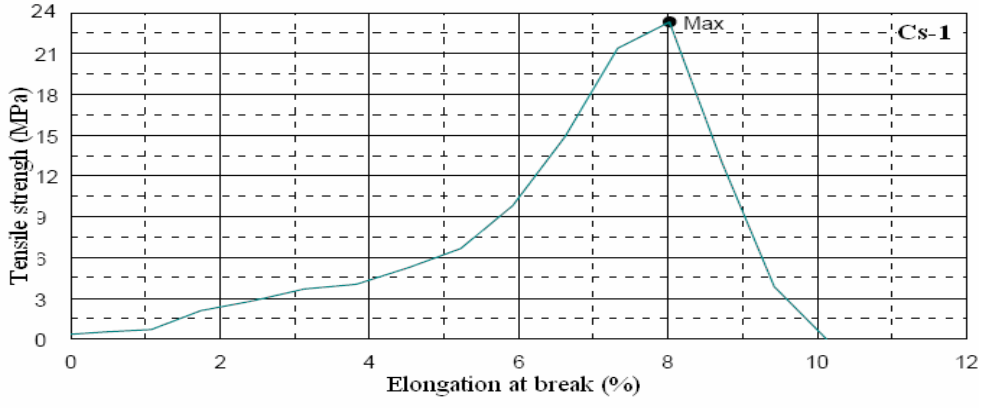

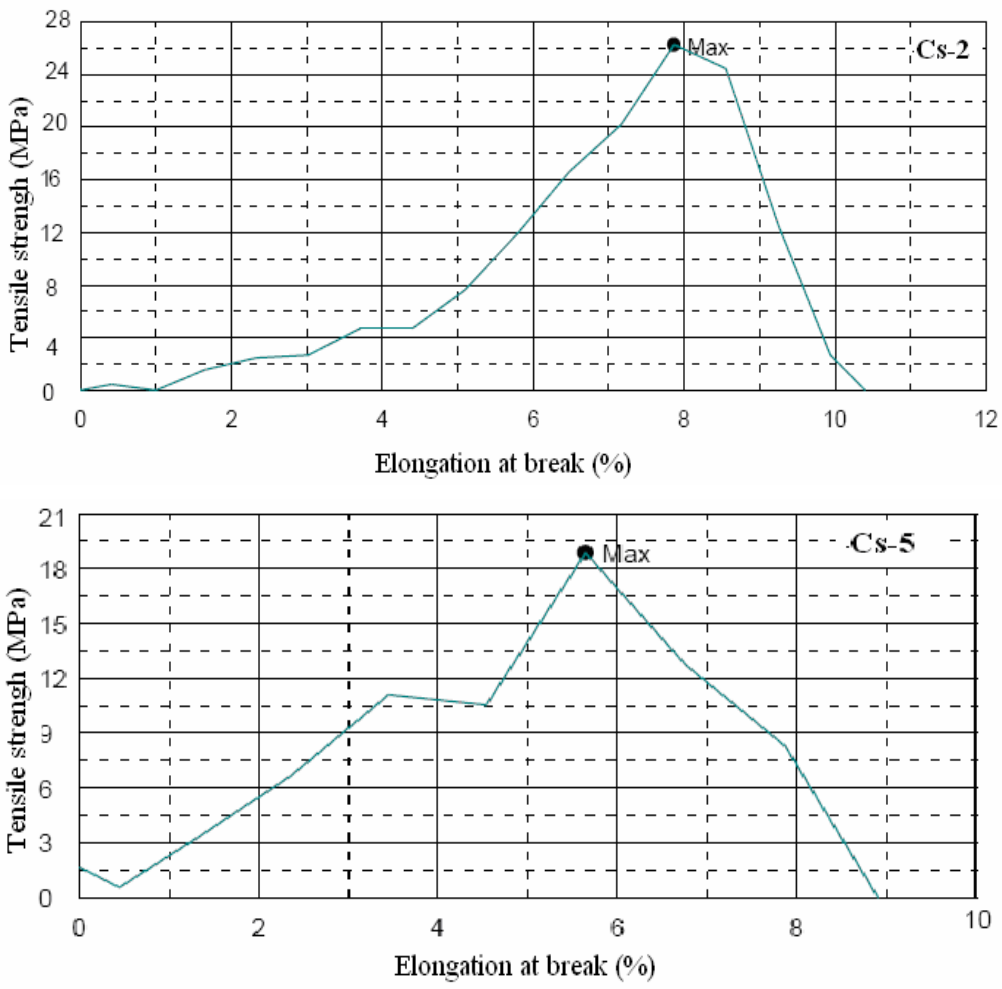

Figure.3.9 Mechanical properties of chitosan and its biocomposite

CHAPTER FOUR

CONCLUSIONS

From SEM analysis, exfoliated composite structures were formed with the addition of small amounts of MMT to the chitosan matrix. Intercalation, together with some exfoliation of chitosan with MMT occurred with increasing the amounts of MMT to 5 wt %.

The FTIR spectra can clearly be seen that all spectra exhibit the presence of characteristic absorptions due to the organic and inorganic groups. FTIR results show that the chitosan molecules and clay particles mainly interact on the surface each other.

The results of TGA showed that the thermal stability of the biocomposites was improved with increase of clay loading in nitrogen flows and air atmosphere. Melting temperature (T_m) and onset temperature of thermal degradation (T_d) of chitosan biocomposite films increased when MMT loading.

The surface roughness increased with the addition of a small amount of clay. Tensile strength of the chitosan film increased with the addition of small amounts of montmorillonite. Elongation-at-break decreased with the addition of clays, but not significantly with addition of MMT.

REFERENCES

ASTM. (1995). In Annual Book of ASTM Standards; *American Society for Testing and Materials:* West Conshohocken, PA,; Vol. 8.01, p 182.

Chitin and Chitosan (2007) from http://www.plasticstrends.net -

Dai J.C., Huang J.T.(1999). Surface modification of clays and clay rubber composite, *Applied Clay Science* 15, 51-65.

Dung P., Milas, M., Rinaudo M. & Desbrieres J.(1994). Water soluble derivatives obtained by controlled chemical modifications of chitosan. *Cerma V-cnrs*, B.P. 53 x. 38041 Grenoble Cedex, France.

Gilman JW. (1999). Synthesis of polymer – montmorillonite nanocomposites by in situ intercalative polymerization. *Applied Clay Science*;15:31.

Marina biopolymers (2007) from http://www.kimica.jp/eng-chitosan-chemi-2.htm

Jill Geddes and Professor Chris Breen (n.d.). *Quantification of swelling materials in rocks using thermogravimetry - mass spectrometry.* Polymers, Composites and Spectroscopy, Materials and Engineering Research Institute, Sheffield Hallam University, Sheffield S1 1WB.

Kittur, F. S., Prashanth, K. V. H., Udaya Sankar, K., & Tharanathan, R. N. (2002). Characterization of chitin and their carboxymethyl derivatives by differential scanning calorimetry. *Carbohydrate Polymers*, 49, 185–193.

Lazaridou, A., & Biliaderis, C. G. (2005). Thermophysical properties of chitosan, chitosan-starch and chitosan-pullulan films near the glass transition. *Carbohydrate Polymers,* 48, 179–190.

Margarita Darder, Montserrat Colilla, Eduardo Ruiz Hitzky; (2003).Biopolymer – clay nanocomposites based on chitosan intercalated in montmorillonite. *Chem.Mater*. Vol:15, 3774-3780.

Okamoto M., (2004). Polymer/Clay Nanocomposites, "Encyclopedia of Nanoscience and Nanotechnology*"* (H. S. Nalwa, Ed.), Vol. 8, p. 1. *American Scientific Publishers, Stevenson Ranch, CA,*.

Newman A.C.D., (1987). *Chemistry of Clays and Clay Minerals*, Mineralogical Society, Monogr. No. 6. Longman, London, Ch. 1, pp. 49-53.

Okamoto, (2005) *Biodegradable Polymer/Layered Silicate Nanocomposites: A Review* Handbook of Biodegradable Polymeric Materials and Their Applications Edited by Surya Mallapragada and Balaji Narasimhan Volume 1: Pages (7-8).

Önal, M., Sarıkaya Y., Alemdaroğlu, T., (2001). Investigation of the Microporous and Mesoporous Structures of the Reşadiye (Tokat/Turkey) Bentonite and its Fractions, *Turkish Journal of Chemistry*, 25, 241-249.

Parfitt, GD (ed.), 1981. Dispersion of Powders in Liquids, *Applied Science Publisher,* NJ.

Ralph E. Grim (1968). *Clay Mineralogy*. New York.

Rieder M, Cavazzini G, D'yakonov YS, Frank-Kamenetskii VA, Gottardi G, Guggenheim S, Koval PV, Müller G, Neiva AMR, Radoslovich EW, Robert J-L, Sassi FP, Takeda H, Weiss Z, & Wones DR (1998) Nomenclature of micas. Clays *Clay Mineralogy*, 46: 586–595.

Mc Graw Hill Book Comp., Ratto, J., Hatakeyama, T., & Blumstein, R. B. (1995). Differential scanning calorimetry investigation of phase transition in water/chitosan systems. *Polymer*, 36(15), 2915–2919.

Sakurai, K., Maegawa, T. T., & Takahashi, T. (2000). Glass transition temperature of chitosan and miscibility of chitosan/poly(n-vinyl pyrrolidone) blends. *Polymer*, 41, 7051–7056.

Seki, Y. (2003). *Adsorption of some herbicides onto organo-clays from aqueous solution*, MSc. Thesis, D.E.U. Graduate Scholl of Natural and Applied Sciences, İzmir Turkey, pp 90.

Sood, A., & Panchagnula, R. (1998). Drug Release evaluation of diltiazem CR preparations, *International Journal of Pharmaceutics* 175, 95-107.

Theng, BKG, (1974).The Chemistry of Clay Organic Interactions, *Wiley,* New York,

Theng, BKG, (1979) Formation and Properties of Clay–Polymer Complexes, *Elsevier*, New York.

Wang SF, Hu Y, Song L, Wang ZZ, Cheng ZY, Fan WC. (2002). Structure–Property Relationship in Chitosan-Based Biopolymer/ Montmorillonite Nanocomposites *Polymer Degradation and Stability*; 77:423.

Yixiang Xu, Xi Ren, Milford A. Hanna. (2006). Chitosan /clay nanocomposite film preparation and characterization. *Journal of Applied Polymer Science,* Vol. 99, 1684- 1691.

Vaia RA, Price G, Ruth PN, Nguyen HT, Lichtenhan. (1999*).* Polymer/layered silicate nanocomposites as high performance ablative materials *Journal of Applied Clay Science*;Vol:15 67-92.

Viseras C., Aguzzi C., Cerezo P.& Lopez Galindo, A. (2006). Uses of clay minerals in semisolid health care and therapeutic products*, Journal of Applied Clay Science*, in press.